Electrocatalysis (2014) 5:396–401
DOI 10.1007/s12678-014-0208-z

Non-precious Metal Oxygen Reduction Reaction Catalysts Synthesized Via Cyanuric Chloride and *N*-Ethylamine

Thiago Lopes · Paulo Olivi

Published online: 21 May 2014

Abstract Non-precious metal oxygen reduction reaction catalysts were synthesized in this study using novel and cheap nitrogen sources, cyanuric chloride, and *N*-ethylamine. These materials presented a promising catalytic activity toward the oxygen reduction reaction (ORR) in acid media, which is the most challenging. For the catalyst based on *N*-ethylamine, the onset potential for ORR is 0.803 V vs reversible hydrogen electrode (RHE) or 0.703 V at 0.1 mA cm^{-2}. The nitrogen source is shown to be extremely important in the final morphology and ORR activity of the catalyst. Steady state ORR polarizations evidenced that the final morphology of the catalysts play a major rule on mass transport in this class of catalysts, with a lamella-like structure being detrimental. Physical characterizations of the catalysts revealed that cyanuric chloride promotes morphology alterations to the carbon support toward a lamella-like structure, while the catalysts synthesized from *N*-ethylamine retained the nanoparticle structure of the carbon precursor. This catalyst exhibited a Tafel slope of 66 mV per current decade in the lower potential region, with promising four-electron selectivity in a polymer electrolyte fuel cell (PEFC) operational potential.

Keywords ORR · PEFC · Cyanuric chloride · *N*-Ethylamine

T. Lopes · P. Olivi
Departamento de Química, Faculdade de Filosofia, Ciências e Letras de Ribeirão Preto, Universidade de São Paulo, Ribeirão Preto, SP 14040-901, Brazil

P. Olivi
e-mail: olivip@ffclrp.usp.br

T. Lopes (✉)
Department of Chemistry, Imperial College, London SW7 2AZ, UK
e-mail: tlopeschem@gmail.com

Introduction

The oxygen reduction reaction (ORR) is remarkably associated with life and energy conversion, constituting a strategic and crucial matter toward economic developments. Therefore, numerous researchers have devoted great attention on developing catalysts for the ORR, aiming at applications such as polymer electrolyte fuel cells (PEFCs) [1–3]. This effort has lead to the development of highly active materials; for instance, Stamenkovic et al. [4] have developed single-crystalline Pt_3Ni catalysts possessing a half-wave potential for the ORR of 0.92 V, and Zhang et al. [5] have developed nanoporous PtNi catalysts presenting a half-wave potential of 0.96 V. However, these catalysts are highly expensive and based on costly metals and, unfortunately, are prone to undergo degradation in strong acidic environments, e.g., PEFC catalyst layers [6].

In parallel to the rich development of noble metal catalysts, there has been a remarkable development of suitable alternatives, with the non-precious metal ORR catalysts (NPMCs) being of great potential to replace the formers [7, 8]. This latter class of ORR catalysts is much less expensive [9, 10], highly active [9], possessing promising longevities in challenging environments, ca. PEFCs [10], and is predominantly synthesized from less expensive metals (e.g., iron), a conductive carbon source, and a nitrogen source such as ammonia and phenantroline [9], polyaniline [10], and others. Although it is generally accepted that both nitrogen and transition metal precursors are necessary to achieve high catalytic activity, the nature of the active site(s) remains a subject of ongoing research and debate [11].

Fully determining the nature of the active site(s) in these non-precious ORR catalysts is crucial toward tailoring the surface density of sites and its activity. To date, some routes was successfully developed, as previously cited, though a lack of knowledge about the nature of the active site(s) hampers a

mandatory breakthrough toward bringing these inexpensive, durable, sustainable, and environment friendly catalyst to viable implementation as ORR materials, for instance, PEFCs, metal-air batteries, chlor-alkali electrolyzers with oxygen-depolarized cathodes, etc. This breakthrough could allow for mass commercialization of devices as PEFCs, where cost is one of the few issues hampering this aim and is mostly caused by the actual state-of-the-art highly expensive noble metal catalysts [12].

Toward determination of the active site, one could think about different approaches, and one of them would be to access how different catalyst precursors can be employed in synthesizing ORR-active catalysts. Along with other approaches, this could allow the rationalization of the rule of each chemical in the synthesis of NPMCs, which, in turn, would be a strong toll in tailoring and wishfully determining the nature of the active site(s). The former is the aim of the present investigation, where fundamentally promising ORR catalysts are proposed. It has been successfully proposed here the use of novel and cheap nitrogen sources, namely, cyanuric chloride and *N*-ethylamine. The carbon source is selected to be the carbon black, grade Monarch 1000 from Cabot Corporation, which presents less micropores and a lower surface area than the traditionally used Ketjen Black or Black Pearls 2000, though allowing the production of highly active ORR catalysts.

Experimental

Synthesis of the Catalysts

The catalysts were synthesized as follows. The carbon source was grade Monarch 1000 from Cabot Corporation with Brunauer–Emmett–Teller (BET) area of 240 $m^2\ g^{-1}$. The nitrogen source consisted of 2,3,6-trichloro triazine (cyanuric chloride) or *N*-ethylamine, both acquired from Sigma-Aldrich. Water-free acetone and ethanol were the solvents for the routes using cyanuric chloride and *N*-ethylamine, respectively.

In a typical route, 0.5 g of carbon black was refluxed in 150 mL of 1.0 mol L^{-1} HCl solution at 80 °C for 24 h, in a water bath, to remove metal traces from the carbon source [10, 13]. After vacuum filtration and washing with plenty of deionized (DI) water (18.2 MΩ/cm), 200 mg of carbon black and approximately 0.0583 mg of $FeCl_3$ (Sigma-Aldrich) and 0.0629 mg of $Co(NO_3)_2$ (Sigma-Aldrich) were added to 100 mL of ethanol and were refluxed for 48 h at 80 °C in a water bath. Next, 2,3,6-trichloro triazine was added, and the solution was allowed to reflux for further 48 h under the same conditions. This nitrogen source was added at two different concentrations to obtain 1:2.3 and 1:6.0 carbon to nitrogen atomic ratios. These refer to catalysts labeled in the text as M1000-23 and M1000-60, respectively. The indexes *a* and *b*, e.g., M1000-23a and M1000-23b, stand for synthesis procedures where the cyanuric chloride is washed out (index *b*, through filtering and rising the final powder material with DI water) or not (index *a*) prior to pyrolysis. When *N*-ethylamine was used (2 mL), the metal cations were complexed with the nitrogen source prior to the first reflux; no second reflux was carried out. Then, the materials were filtered and washed with DI water and were dried in an oven at 105 °C for 24 h. The dried powders were heat-treated in a tubular oven at 900 °C under nitrogen atmosphere for 1 h, using a heating ramp of 20 °C min^{-1}. Finally, the catalysts were refluxed in 100 mL of 0.5 mol L^{-1} H_2SO_4 at 80 °C for 24 h to remove undesired metal oxides.

Electrochemical Characterization

The catalysts were characterized by electrochemical techniques. In every experiment, a 0.5 mol L^{-1} H_2SO_4 solution was used as an electrolyte at room temperature (25±2 °C). A gold mesh served as a counter electrode. Ag/AgCl (3 mol L^{-1} NaCl) served as a reference electrode, although potentials herein refer to the reversible hydrogen electrode (RHE). This was possible by frequently monitoring the potential of the Ag/AgCl (3 mol L^{-1} NaCl) electrode against that of a freshly prepared RHE. A rotating disk electrode (AFE2M050GC from Pine Research Instrumentation) was used to test the catalysts by the thin-film rotating disk electrode (RDE) technique [14]. The entire electrochemical characterization of the non-precious catalysts was accomplished using a catalyst loading of 0.75 mg catalyst cm^{-2} disk, having 40 wt% of Nafion™; the reference catalyst or platinum (Pt/C-XC72 50 wt% in metal from Fuel Cell Earth LLC) had a loading of 60 μg Pt cm^{-2} disk. As a routine, the catalysts on the RDE electrodes had the potential cycled between 0.05 and 1.05 V vs RHE through cyclic voltammetry. The objective of this cycling was twofold: to verify the surface electrochemistry of the catalysts and to conduct conditioning, under a rotation speed of 900 rpm, in nitrogen-saturated solutions. To assess the catalytic activity of the catalysts toward the ORR, steady state polarization curves were recorded between 0.95 and 0.075 V vs RHE under a potential step of 30 mV and step duration of 30 s, in O_2-saturated solutions. The rotation speeds were varied between 400 and 2,500 rpm. A potentiostat/galvanostat Autolab model PGSTAT30 was used for all the experiments. The current densities in all graphs, unless indicated, are plotted vs the geometric area of the RDE electrode (0.196/cm^2).

Physical Characterization

Energy-dispersive X-ray spectroscopy (EDX) analyses were performed on a microscope Leica-Zeiss LEO 440 SEM model coupled to an Oxford 7060 analyzer. X-ray diffraction (XRD)

patterns were obtained on a Siemens D5005 apparatus operating with CuKα radiation (λ=1.54056 Å).

Results and Discussion

Figure 1 illustrates a typical catalytic activity of the synthesized catalysts toward the ORR; the inset shows the performance gap (in half-wave potential) between the M1000-FeCo-NEA and the state-of-the-art PEFC Pt/C catalyst. The acronyms for the name of the catalysts stand for the different nitrogen sources employed during their synthesis, where NEA stands for *N*-ethylamine; all others correspond to cyanuric chloride. In the former cases, the different catalysts represent different nitrogen to carbon molar ratios employed during synthesis. It is clear based on this results that the ratio of carbon to nitrogen employed during catalyst synthesis along with the chemical nature of the nitrogen precursor is of crucial importance. These results show that catalysts synthesized under a lower C:N ratio or the M1000-23 (1:2.3) and M1000-FeCo-NEA (1:1.5) exhibit a higher catalytic activity for the ORR, disregarding the nitrogen precursor employed.

The cyclic voltammograms of the catalysts in N_2-saturated 0.5 M H_2SO_4 solution are mostly featureless, even though they are different. The catalysts synthesized with *N*-ethylamine (Fig. 2a) present similar features to the carbon black precursor (inset in Fig. 2) or the redox couple quinine/hydroquinone [15]. On the other hand, the catalysts synthesized from cyanuric chloride exhibit a redox couple (Fig. 2b) that could represent the Fe^{III}/Fe^{II} redox couple, as reported in the literature [16].

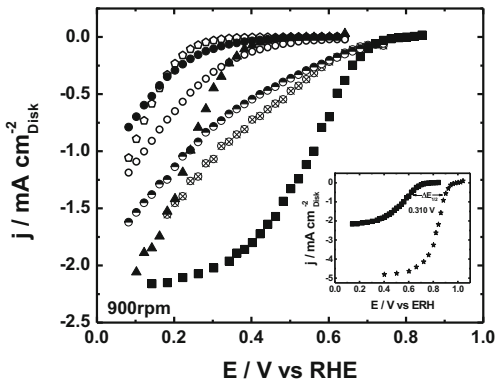

Fig. 1 Steady state ORR polarization plots of catalysts synthesized, as a function of the RDE rotation speed (in rpm), in an O_2-saturated 0.5 M sulphuric acid electrolyte. Glassy carbon disk is 5 mm in diameter. Catalyst loading is 0.75 mg cm^{-2}, except for Pt/C, 60 μ Pt cm^{-2}. Electrolyte temperature is 25 °C. *Inset* indicates half-wave potential difference between M1000-FeCo-NEA and a standard PEFC platinum catalyst 50 % Pt/C (Fuel Cell Earth LLC). *Symbols* stand for the following: *pentagon*, glassy carbon; *filled circle*, M1000-60a; *empty circle*, M1000-60b; *crossed out circle*, M1000-23a; *half-filled circle*, M1000-23b; *filled triangle*, Monarch 1000; *filled square*, M1000-FeCo-NEA; and *filled star*, Pt/C

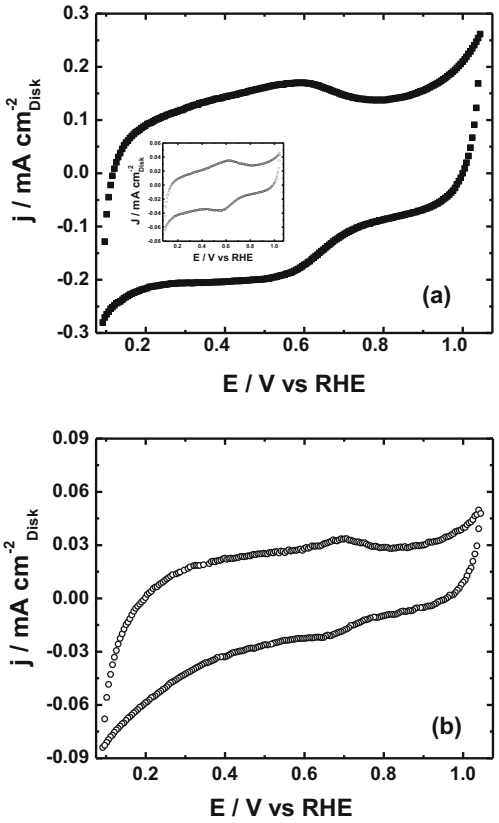

Fig. 2 Cyclic voltammograms of catalysts: **a** M1000-FeCo-NEA and the carbon back precursor, Monarch 1000 (*inset*), and **b** M1000-60b in N_2-saturated 0.5 M sulfuric acid electrolyte. Non-stationary speed is 900 rpm. Catalyst loading is 0.75 mg cm^{-2}. Scan rate is 10 mV s^{-1}. Electrolyte temperature is 25 °C

Figure 3 depicts steady state ORR polarization plots for the catalyst prepared with *N*-ethylamine, as a function of the RDE rotation speed in an O_2-saturated 0.5 M sulfuric acid solution.

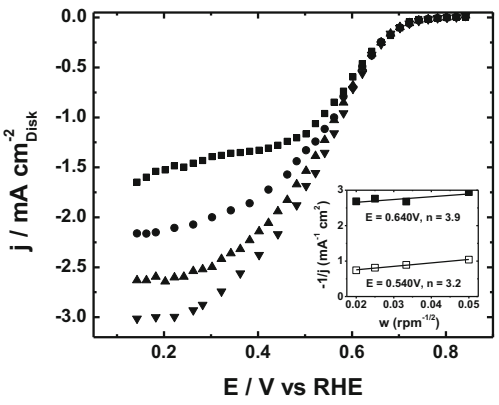

Fig. 3 Steady state ORR polarization plots for the M1000-FeCo-NEA catalyst as a function of RDE rotation speed (in rpm), in an O_2-saturated 0.5 M sulphuric acid electrolyte. *Inset* indicates Koutecky-Levich plots for the ORR on the M1000-FeCo-NEA catalyst at different electrode potentials. Catalyst loading is 0.75 mg cm^{-2} disk. Electrolyte temperature is 25 °C. Symbols stand for the following: *filled square*, 400 rpm; *filled circle*, 900 rpm; *filled triangle*, 1,600 rpm; and *filled inverted triangle*, 2,500 rpm

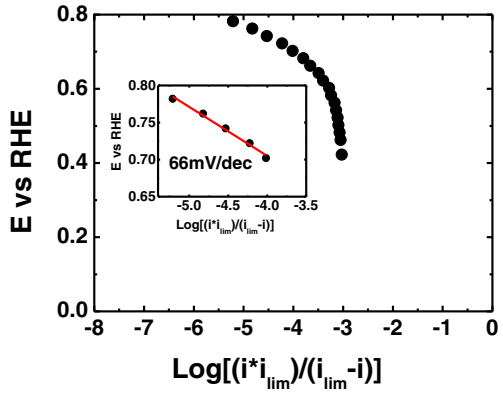

Fig. 4 Tafel plot for the ORR measured for the M1000-FeCo-NEA at 900 rpm under steady state polarization, in O_2-saturated 0.5 M H_2SO_4 electrolyte at 25 °C

The onset potential for the *N*-ethylamine-based catalyst is high at 703 mV vs RHE and similar to the cyanuric chloride-based M1000-23 catalysts (Fig. 1). Though, the latter catalysts do not exhibit similar ORR activity compared to the former, potentially due to mass transport of reactants and products being hampered by the lamella-like morphology of the material, later highlighted by SEM analysis. Here, the onset potential is defined as the potential required to generate an ORR current density of 0.1 mA cm^{-2} in a steady state RDE experiment [10]. If the potential obtained upon crossing from positive to negative currents is considered as the onset potential, then 803 mV vs RHE should be considered instead. However, it is a safer option to use the former definition of onset potential. The inset of Fig. 3 illustrates the four-electron selectivity of the M1000-FeCo-NEA non-precious catalyst. At low overpotentials, this catalyst is more selective toward the desirable four-electron ORR pathway, with a high electron transfer number of 3.9 at PEFC operational potentials.

Additional data analysis reveal differences in the Tafel slope for the oxygen reduction on the M1000-FeCo-NEA catalyst at low overpotentials (Fig. 4) compared to that at high overpotentials, being 66 mV per current decade in the former region. This value agrees with literature data on cobalt and iron-based non-precious catalysts [10, 16]. For these

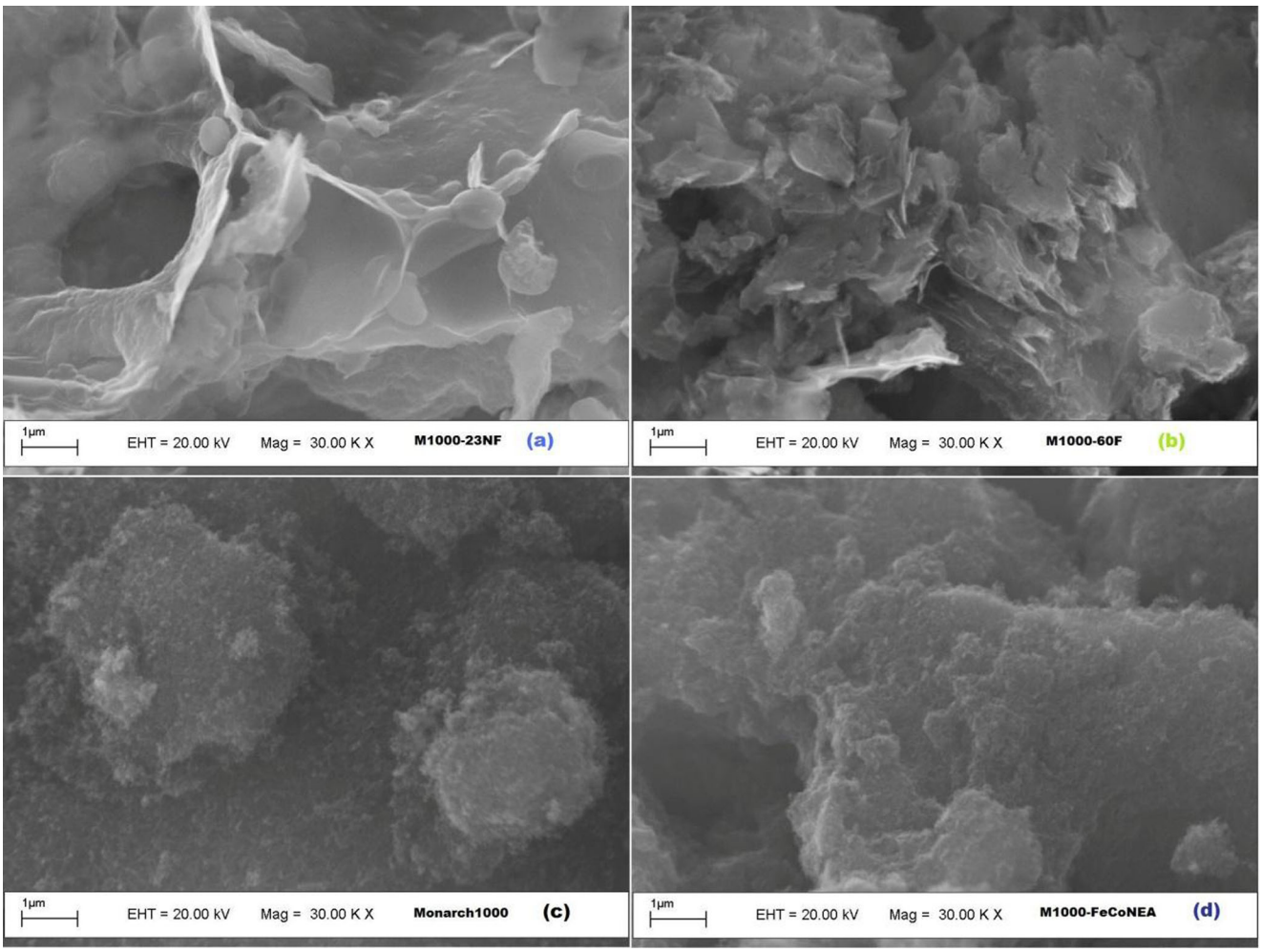

Fig. 5 SEM images of selected catalysts: **a** M1000-23a, **b** M1000-60b, **d** M1000-FeCo-NEA, and **c** the carbon black precursor—Monarch 1000

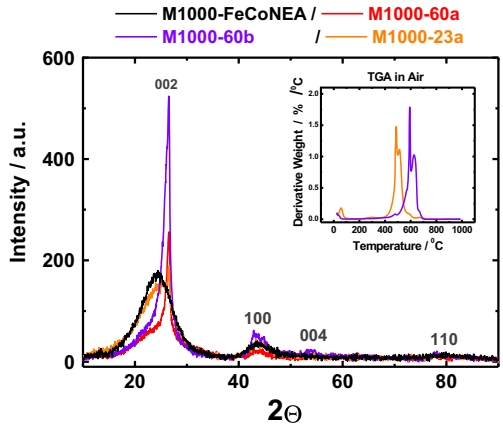

Fig. 6 XRD patterns of selected catalysts with thermogravimetric analysis (*inset*)

materials, the ORR mechanism at low overpotentials is suggested to involve a simple mediation by the Fe^{III}/Fe^{II} redox couple, while concerted charge transfer and oxygen–oxygen bond splitting are to occur at higher overpotentials. In this region, the Fe^{II} is the stable iron species, and oxygen interacts directly with this rather than with Fe^{III} [16]. A larger Tafel slope at high overpotentials (>240 mV per current decade) originates from intrinsic features of the ORR mechanism rather than from incomplete catalyst utilization or uncompensated resistance in the catalyst layer [16]. This is cited, once high catalyst loadings on RDEs/RRDEs are usual in the field of non-precious ORR catalyst. These are reinforced by the fact that the reaction order for oxygen remains equals to one on non-precious ORR catalysts along a typical ORR potential window [16], as per the present work.

Physical characterization of the catalysts was performed to gain insight into their structure and elemental composition. Figure 5 contains SEM images of some of the synthesized catalysts. The change in the Monarch 1000 morphology for the catalysts prepared with cyanuric chloride is clear, while the catalyst obtained from NEA apparently retain the nanoparticle structure of the carbon black precursor. Cyanuric chloride completely changes the morphology of the precursor to a lamella-like structure, diminishing the surface area of the catalyst. This is supported by the XRD pattern of these catalysts (Fig. 6); the cyanuric chloride-based catalyst displays a sharper peak in the graphite-like structure region (002 plane). Based on data in Fig. 1, this lamella-like structure is possibly responsible for the mass transport issues observed on the ORR plots for the M1000-23 catalysts, which exhibit high onset potentials, though clearly suffer from mass transport. This result highlights a fact commonly missed in this field or the importance that morphology may play on the ORR polarization response of non-precious catalysts due to the transport of reactant and products transport at the active site(s), which is to be more severe and evident in acid environments.

EDX assisted in determining the elemental composition of the catalysts. Table 1 presents the elemental composition of some catalysts along with the ORR onset and half-wave potential for the M1000-FeCo-NEA catalyst. The former catalyst, which presented the higher catalytic activity toward the ORR, interestingly possesses the smallest amount of metal. However, it is noteworthy to discuss that an onion-like structure reported by Wu et al. [10] could hamper detecting metals in these types of carbon catalysts. In these materials, graphene sheets are prone to encapsulate metal nanoparticles, making them difficult to detect by EDX, as observed through XPS in the literature [17].

Figure 6 brings XRD and thermogravimetric analysis data for some of the catalysts synthesized using *N*-ethylamine and cyanuric chloride. Judging from the Bragg reflection of the (002) peak [18], the most active catalysts (M1000-23 and M1000-FeCo-NEA) exhibit a broader peak, corresponding to a larger interlayer distance, which is corroborated by TGA data, where the less graphitic structure is more prone to

Table 1 EDX elemental analysis of selected catalysts synthesized, with additional half-wave and onset potentials vs RHE for the M1000-FeCo-NEA

	M1000-23a		M1000-60b		Monarch 1000		M1000-FeCo-NEA[a]	
	at%	wt%	at%	wt%	at%	wt%	at%	wt%
Atom [a]								
C	89.90	85.90	95.30	93.00	92.00	89.10	94.30	91.80
O	9.40	12.00	4.40	5.75	7.50	9.70	5.10	6.60
Fe	0.20	0.70	0.15	0.80	0.06[b]	0.03[b]	0.01[b]	0.08[b]
Half-wave potential (V)								0.572
Onset potential (V)								0.803
Onset potential (V) at 0.1 mA cm^{-2}								0.703

[a] Cobalt not detected

[b] Values below the detection limit of the equipment

undergo oxidation by oxygen. On the other hand, catalysts synthesized via cyanuric chloride display a positive shift of the diffraction position, higher intensity, and narrower line width of the (002) peak and thus are more graphitic. A higher degree of graphitization has been shown to denote a lower BET surface area in ORR electrocatalysts based on carbon materials [19]. Therefore, a higher degree of graphitization of the catalysts synthesized via cyanuric chloride might denote a lower surface area of the material and, thus, a lower surface density of active sites. This would reflect in a lower ORR mass activity of the catalysts synthesized via cyanuric chloride when compared to the higher activity of the less graphitic catalysts synthesized via *N*-ethylamine. The peak centered at 2θ around 43°–44° lies in a region where Fe, Fe_2O_3, Co_3O_4, and graphite (002) exist. Wu et al. [10, 20] proposed that this could also contemplate $Fe(Co)S_x$ nanoparticles in the case of similar catalysts. This hampers further analysis of the metal.

The catalytic activity of the M1000-FeCo-NEA and the M1000-23 toward the ORR is shown to be promising, remarkably considering the low surface area of carbon black precursor utilized in the present investigation. The cheap cyanuric chloride-based non-precious catalysts have proven to be a promising alternative toward investigating morphology and producing highly active materials.

Conclusion

Non-precious ORR catalysts were synthesized using novel sources of nitrogen, namely, 2,3,6-trichloro triazine (or cyanuric chloride) and *N*-ethylamine (NEA), with Monarch 1000 from Cabot Corporation as the carbon source. The catalysts resulting from cyanuric chloride generated undesired lamella-like morphologies, though presenting promising ORR activities. On the other hand, the catalysts resulting from NEA retained the morphology of the precursor carbon black with higher activities toward the ORR. The four-electron selectivity of the NEA-based catalysts is promising in the voltages of operating PEFCs, with around 3.9 electrons per oxygen molecule. In the lower overpotential region, the NEA-based catalysts give a Tafel slope of 66 mV per current decade. The nitrogen source plays a key role in the morphology and ORR activity of the catalyst, with active sites possibly been similar to those on catalysts synthesized via more expensive nitrogen precursors found in the literature. Under the presented experimental conditions, NEA-based catalysts perform better toward the ORR, with an onset potential of 0.803 V vs RHE or 0.703 V vs RHE at 0.1 mA cm^{-2}.

Acknowledgments Authors thank FAPESP for financial support, grant #2009/17158-0 (from 2010 to 2011). We also thank Alexandre G. Carmello from Cabot Corp. of Brazil for valuable information on the physical chemistry of Cabot carbon blacks as well as Cabot Corp. of Brazil for providing free samples.

References

1. M.K. Debe, Electrocatalyst approaches and challenges for automotive fuel cells. Nature **489**, 43–51 (2012)
2. E.N. Gribov, A.Y. Zinovieva, I.N. Voropaev, P.A. Simonov, A.V. Romanenko, A.G. Okunev, Activities of Pt/Sibunit-1562 catalysts in the ORR in PEMFC: effect of Pt content and Pt load at cathode. Int. J. Hydrog Energy **37**, 11894–11903 (2012)
3. R.R. Adzic, J. Zhang, K. Sasaki, M.B. Vukmirovic, M. Shao, J.X. Wang, A.U. Nilekar, M. Mavrikakis, J.A. Valerio, F. Uribe, Platinum monolayer fuel cell electrocatalysts. Top. Catal. **46**, 249–262 (2007)
4. V.R. Stamenkovic, B. Fowler, B.S. Mun, G. Wang, P.N. Ross, C.A. Lucas, N.M. Markovic, Improved oxygen reduction activity on $Pt_3Ni(111)$ via increased surface site availability. Science **315**, 493–497 (2007)
5. J. Zhang, K. Sasaki, E. Sutter, R.R. Adzic, Stabilization of platinum oxygen-reduction electrocatalysts using gold clusters. Science **315**, 220–222 (2007)
6. T.R. Ralph, M. Hogarth, Catalysis for low temperature fuel cells part I: the cathode challenges. Platin Met Rev. **46**, 3–14 (2002)
7. L.Y. Johansson, R. Larsson, Electrochemical reduction of oxygen in sulfuric acid catalyzed by porphyrin-like complexes. J. Mol. Catal. **38**, 61–70 (1986)
8. S. Gupta, D. Tryk, I. Bae, W. Aldred, E. Yeager, Heat-treated polyacrylonitrile-based catalysts for oxygen electroreduction. J. Appl. Electrochem. **19**, 19–27 (1989)
9. M. Lefèvre, E. Proietti, F. Jaouen, J.P. Dodelet, Iron-based catalysts with improved oxygen reduction activity in polymer electrolyte fuel cells. Science **324**, 71–74 (2009)
10. G. Wu, K.L. More, C.M. Johnston, P. Zelenay, High-performance electrocatalysts for oxygen reduction derived from polyaniline, iron, and cobalt. Science **22**, 443–447 (2011)
11. J.P. Dodelet, The controversial role of the metal in Fe- or Co-based electrocatalysts for the oxygen reduction reaction in acid medium, in *Electrocatalysis in fuel cells*, ed. by M. Shao, vol. 9 (Springer, London, 2013), pp. 271–338
12. H.A. Gasteiger, N.M. Markovic, Just a dream or future reality? Science **324**, 48–49 (2009)
13. G. Wu, Z. Chen, K. Artyushkova, F.H. Garzon, P. Zelenay, Polyaniline-derived non-precious catalyst for the polymer electrolyte fuel cell cathode. ECS Trans. **16**, 159–170 (2008)
14. T.J. Schmidt, H.A. Gasteiger, R.J. Behm, Rotating disk electrode measurements on the CO tolerance of a high-surface area Pt/vulcan carbon fuel cell catalyst. J. Electrochem. Soc. **146**, 1296–1304 (2009)
15. K. Kinoshita, J.A.S. Bett, Potentiodynamic analysis of surface oxides on carbon blacks. Carbon **11**, 403–411 (1973)
16. J. Chlistunoff, RRDE and voltammetric study of ORR on pyrolyzed Fe/polyaniline catalyst. On the origins of variable Tafel slopes. J. Phys. Chem. C **115**, 6496–6507 (2011)
17. T. Onodera, S. Suzuki, T. Mizukami, H. Kanzaki, Enhancement of oxygen reduction activity with addition of carbon support for non-precious metal nitrogen doped carbon catalyst. J. Power. Sources **196**, 7994–7999 (2011)
18. J. Yan, T. Wei, B. Shao, F.Q. Ma, Z.J. Fan, M.L. Zhang, C. Zheng, Y.C. Shang, W.Z. Qian, F. Wei, Electrochemical properties of graphene nanosheet/carbon black composites as electrodes for supercapacitors. Carbon **48**, 1731 (2010)
19. S. Zhang, M.S. Miran, A. Ikoma, K. Dokko, M. Watanabe, Protic ionic liquids and salts as versatile carbon precursors. J. Am. Chem. Soc. **136**, 1690–1693 (2014)
20. G. Wu, K. Artyushkova, M. Ferrandon, A.J. Kropf, D. Myers, P. Zelenay, Performance durability of polyaniline-derived non-precious cathode catalysts. ECS Trans. **25**, 1299–1311 (2009)